Influence of Fuselage Shape on Single Fin Buffeting

T R Chesneau and N J Wood
School of Mechanical Engineering,
University of Bath.
Bath, Avon. BA2 7AY, UK

Abstract

The effect of fuselage shape on the fin buffeting characteristics of a generic single fin combat aircraft has been investigated experimentally. Tests have been completed in the University of Bath 2.1mx1.5m low speed wind tunnel using an instrumented model. Fin buffeting response data and fin surface pressures have been recorded for angles of attack up to 55° with flow geometry studied using laser light sheet flow visualisation. The forebody vortices have been shown to draw the wing vortex inboard and advance the onset of fin buffeting. This modifies the relationship between angle of attack and the characteristic frequency of the unsteady flow which, in turn, may change the magnitude of the fin buffeting.

Nomenclature

$\bar{\bar{c}}$	Aerodynamic mean chord
f	Frequency, Hz
m	Fin generalised mass in mode
n_m	Modified reduced frequency parameter $n_m = \frac{f\bar{\bar{c}}\sin\alpha}{U_\infty}$
$\bar{p}$	RMS unsteady pressure
q	Free stream dynamic pressure
S	Fin Reference area
U_∞	Freestream Velocity
$\ddot{z}$	RMS fin tip acceleration in mode
$\sqrt{nG(n)}$	Buffet excitation parameter
α	Angle of Attack, degrees
ζ	Total damping ratio of fin as a % of critical
PSD	Power Spectral Density function
RMS	Root Mean Square

Introduction

Significant changes in air combat are occurring with the development of new aircraft and weapons technologies[1]. There is increased interest in reducing the radar observability of modern combat aircraft to provide a tactical advantage over an adversary in the initial stages of 'beyond visual range' combat. As the combat scenario develops, low radar observability becomes less important and agility over an adversary is paramount[2]. Rapid manoeuvring flight during close quarters combat is characterised by transient flow conditions around the aircraft and extensive regions of highly separated flow. In addition, the use of 'novel' aircraft shapes (e.g. B-2, F-117) to reduce the radar cross section of the aircraft may result in separated flow throughout a large proportion of the flight envelope and unfamiliar unsteady aerodynamics.

An aircraft immersed in unsteady flow may experience aerodynamic loading (**buffet**), either as wideband 'white noise' excitation or as randomly occurring bursts of periodic loading. Under certain flight conditions and geometric configurations, the buffet loading may induce a significant dynamic response on the aircraft (**buffeting**) occurring as a rigid body mode causing a degradation in the handling characteristics[3] or the excitation of some flexible part of the aircraft[4][5].

An example of such an aerodynamic/structural interaction is the phenomenon of fin buffeting[6], where the vortices resulting from separated flows over the wing and upstream components impinge on the fin surfaces, inducing a dynamic response. Under certain flight conditions and geometric configurations the magnitude of the response may be large which is detrimental to the fatigue life of the fin and attachment structure. This is clearly undesirable and may result in in-service repair or replacement modifications or in severe circumstances a reduction of the flight envelope. Problems with fin buffeting were encountered soon after the F/A-18 entered operational service, and modifications have included a leading edge fence to alter the flowfield and substantial structural reinforcement of the fin attachment in order to reduce the response of the fin and increase the fatigue life at critical flight conditions[7]. Modification such as these are both costly and may lead to customer dissatisfaction with the aircraft.

As the angle of attack of a delta wing increases, vortices emanating from the leading edge grow in size and strength, until, at some point the vortices will undergo a sudden transformation known as vortex breakdown or burst, described as the sudden change in state from a highly organised vortical structure to a disorganised swirling turbulent flow[8]. It is well documented that this burst vortical flow exhibits distinct periodic oscillations with a frequency which is a function of free stream speed and a length scale[9]. For a fixed streamwise distance in the wake of vortex breakdown, the dominant

frequency within the excitation can be expressed in terms of a modified non-dimensional frequency parameter, n_m, for any given wing planform[10][11].

$$nm = \frac{f \bar{c} \sin\alpha}{U\infty}$$

This frequency parameter represents a correlation between the angle of attack and the motion of the vortex burst over the wing. Figure 1.1 shows the variation of the modified reduced frequency parameter with wing sweep[12] showing that n_m is a unique function of wing sweep (or more globally, wing planform).

For a given angle of attack, the maximum possible fin response occurs when a dominant frequency in the excitation is matched to a fin modal frequency[7]. If the excitation is detuned, either by a change in test speed, or a change in n_m, then a reduction in response will take place. The addition of components upstream of the wing, including leading edge extensions, foreplanes or the fuselage itself, can modify the response of the fin in two ways. The additional unsteady flow can directly interact with the fin or may integrate with the strong wing vortex to modify the frequency content or the vortex position, thus effectively modifying n_m.

During the initial conceptual stage of aircraft design, when the geometric configuration is under investigation, initial estimates must be made to ensure sufficient structural strength throughout the entire flight envelope. This is especially true during combat manoeuvres where the aircraft is subject to large dynamic loads, for example high rate pitch up manoeuvres or stores release. The unsteady flow developed throughout the flight envelope may result in aircraft loads which differ in both frequency and magnitude to those defined for other dynamic loads, whether this be the result of wing, excrescence or fin buffeting, and it is important that the aircraft components are acceptable in terms of their structural integrity,

Forebody features or excrescence's on an aircraft may result in the formation of complex separated flows, the form of which is dependent on the geometry and flight conditions. As the shape of the aircraft becomes less familiar to aerodynamicists, typical of the low radar observability design requirement, so follows the inability to predict the flowfield with confidence. In the absence of detailed information regarding the flowfield, it is necessary to make initial estimations of the fin buffeting characteristics and make inputs into the geometric design process to minimise problems as the design matures.

Investigations have been completed into the effect of alternative fuselage and forebody shapes on the fin buffeting response of a generic single fin combat aircraft. Unsteady pressures on the fin have been measured and related to the fin response measured using an instrumented flexible fin. Laser light sheet flow visualisation has been used to supplement the pressure data acquired on the fin and determine the vortex interactions as the angle of attack increases. The objective of the experimental work is to develop an understanding of the interaction of the unsteady flow developed around a novel configuration with the fin. The aim is to develop a design tool for the prediction of fin buffeting problems in the early conceptual design phase of an aircraft.

Experimental details

The baseline wind tunnel model used for the testing is shown in figure 2.1 This model is representative of a low wing generic single fin combat aircraft. It consists of a 60° cropped delta wing with a rounded leading edge, attached to a rounded edge, square section fuselage and a tangent ogive nose. This baseline model can be modified with the addition of a number of alternative fuselage shapes illustrated in figure 2.2 These were produced in two sections. The constant cross section fuselage shapes were produced by British Aerospace wind tunnel model department, CNC machined from solid mahogany. The complex forebody shapes were produced using a computer controlled stereo lithography process[13].

In order to measure the fin buffeting response to the unsteady flowfield, the model was equipped with a flexible fin illustrated in figure 2.3. The fin comprised an aluminium spar mounted with a fin tip accelerometer and root strain gauges and was covered by an aerodynamic shroud constructed from segmented balsa wood. The fin was dynamically scaled using the reduced frequency, n_m, such that the characteristic frequency of the wing vortices (as a function of angle of attack, tunnel speed and model size) coincided with the natural frequency of the fin in the first bending mode. The free stream speed was maintained as high as possible to ensure a high signal to noise ratio and thereby an acceptable level of repeatability.

An alternative rigid fin is shown in figure 2.4. Pressure tappings on both the port and starboard sides of the fin enabled the unsteady pressure flowfield around the fin to be measured. The tappings were uniformly distributed along the length of the fin at 5% of the local chord from the leading edge.

The fin pressure tappings were drilled into steel hypodermic tubes on the port and starboard sides of the fin and coupled to two miniature pressure transducers to acquire port and starboard signals simultaneously. The unused tappings were masked off, enabling acquisition

of data at one fin location at one time. Each tapping was individually dynamically calibrated using test apparatus capable of produced oscillatory pressures of varying frequency, up to 500Hz. The tube transfer functions were applied to the Power Spectral Densities of the acquired time histories enabling the frequency content and amplitude of the original flowfield to be determined.

The testing was completed in the main wind tunnel at the University of Bath. This a closed circuit wind tunnel with the fan positioned downstream of the 2.1mx1.5m (7'x5') test section. The test section incorporates glass panels in the floor and wall to provide optical access for laser light sheet flow visualisation. The model was mounted in the test section as in figure 2.5, on a high angle of attack pantograph mechanism which allowed the angle of incidence to be varied from 0° to 90°. Since the data consists of comparisons of configurations at similar angles of attack, no account of blockage effects have been included.

The wind tunnel speed was set to maximise the peak buffeting response of the fin in the low wing baseline configuration. The reduced frequency parameter defined a tunnel speed to tune the characteristic frequency of the wing vortex to the fin first bending natural frequency at the peak buffeting angle of attack. This provided a tunnel speed of approximately 20m/s, which was subsequently verified experimentally to result in maximum response.

The buffet and buffeting time histories were monitored by a PC based data acquisition system from Data Translation™ and analysed using a series of specifically written programs. The buffeting data from the accelerometer and the strain gauges on the flexible fins were acquired at a rate of 512 samples/second for 30 seconds around buffet onset and 60 seconds around the peak buffeting condition. This has been shown to produce data repeatability better than 3% for the buffeting data. The data were reduced using the AGARD buffet excitation parameter[14] which represents the generalised force acting on the fin, derived from the structural response. It is calculated from the fin tip acceleration by:

$$\sqrt{nG(n)} = \frac{2}{\sqrt{\pi}} \frac{m\ddot{z}}{qS} \sqrt{\zeta}$$

Port and starboard unsteady pressure data were acquired at a rate of 1024 samples/second for 30 seconds for each of the six tappings on the fin for a range of angles of attack. This provides a data repeatability better than 2%. The data were processed in the sequence shown in figure 2.6. An ensemble averaged FFT of the time history was completed producing a frequency resolution of 2Hz, to which the tapping pressure calibration with respect to frequency was applied. This was converted to a power spectral density from which the RMS of the signal was obtained.

Results and Discussion

Low wing baseline fin buffeting

Figure 3.1 shows the vortex flow features for the baseline, low wing square section fuselage, configuration. This figure was created by compiling eleven independent images from laser light sheet flow visualisation to allow high contrast of the flow features. Highlighted are the forebody vortex emanating from the nose of the model and tracking streamwise along the fuselage and the wing vortex growth with streamwise position. As the angle of attack is increased, the size and strength of both the forebody and wing vortex increases.

Figure 3.2 shows the starboard RMS unsteady pressure at tapping 1 towards the fin root and tapping 6 toward the fin tip (as shown in figure 2.4). The magnitude of the unsteady pressure measured at tapping 1 is significantly lower than that observed at the fin tip above 35° angle of attack. As the angle of attack is increased and the vortices grow in size and strength, the vortical shear layers will impact the fin. This represents the first observance on unsteady pressure on the fin at 32° angle of attack. This unsteady pressure excites a response of the fin as shown in figure 3.3 corresponding to the buffeting onset condition. As the angle of attack is increased, the vortices track inboard and upwards imparting increased excitation on the fin. A critical condition is reached when the shear layers meet at the fin tip (near tapping 6) and maximum excitation is observed on the fin as in figure 3.2. As a function of the vortex amplitude and frequency, the peak buffeting condition highlighted in figure 3.3 is reached. As the shear layers are removed from the critical condition, upwards and away from the fin, the excitation, and hence the response decays. This is the post buffeting condition.

Figure 3.4 shows the spectra of the starboard unsteady pressure at tapping 6 for the low wing baseline configuration and angles of attack at a low fin buffeting response level, peak buffeting and post buffeting conditions. This figure is plotted as a power spectral density of the unsteady pressure (PSD) against frequency in Hz. As the angle of attack of the model is increased, the dominant frequency of the unsteady flow on the fin reduces. This change in characteristic frequency with angle of attack is modelled by the reduced frequency parameter, n_m. At the condition of peak excitation where the wing vortex shear layers impinge at the fin tip, the unsteady excitation is centred around a frequency of 36Hz. This corresponds to the first bending modal frequency of the fin. Fin buffeting can be considered as a simple mechanical system, with the unsteady pressures

as an input loading, the fin as a filter, and the fin response as the output. The maximum possible response at any condition will occur when the excitation is tuned to a fin natural mode. For the low wing baseline condition, this occurs at the condition of maximum excitation, hence the observed response in figure 3.3 is the maximum possible for this geometry.

A change in the characteristic frequency at the conditions of peak excitation will result in a reduction of the magnitude of the fin buffeting response, as the system becomes detuned. This is evidenced by figure 3.5, showing the effect of both a speed increase and decrease on the fin buffeting response. A change in speed will detune the flow excitation from the fin modal frequency resulting in reduced fin buffeting response levels compared to the tuned condition. Of interest is the buffet onset condition which, being largely unaffected by changes in test speed, demonstrates that this condition is flow geometry related. At larger angles of attack the frequency content of the flowfield becomes important as the fin becomes immersed in the vortex shear layers. Figure 3.6a shows PSD's of the unsteady pressures at the critical condition where the vortex shear layers meet at the fin tip for the three test speeds. As the test speed increases, the characteristic frequency is increased. Replotting this figure as reduced frequency parameter, figure 3.6b, it can be seen that the frequencies are represented by a reduced frequency parameter, n_m of approximately 0.55.

The importance of tuning the response to the input signal has been demonstrated and is of concern with regard to flight test results. Under a test flight condition, the fin buffeting response could fall well within structural limits if the configuration were not in the tuned condition. If the speed were to vary in order to tune the flowfield with the fin modes, large, potentially damaging increases in the fin response could occur. In a similar way, if the flow is tuned at a flight condition where the magnitude of excitation is small, there could be a condition, where the flowfield is slightly detuned, but under conditions of greatly increased excitation. There is clearly a trade-off between the amplitude of the unsteady flow and the frequency compared to a natural mode. In summary three conditions must be satisfied for the occurrence of fin buffeting

- Geometry - An unsteady pressure flowfield must contact the fin in order to excite a response. The geometry of the configuration determines the buffeting onset, where the unsteady flow first makes contact with the fin. It also determines the angle of attack of the critical condition for peak buffet.
- Frequency - The maximum fin buffeting response at any condition will occur when the frequency of excitation is matched to the fin natural mode.
- Magnitude - The magnitude of the unsteady pressures on the fin and the way they are spatially and temporally correlated between the port and starboard surfaces influences the magnitude of the fin buffeting response.

Further studies using two surface mount pressure transducers have shown that the magnitude of the unsteady pressure on the fin is reduced with increasing chordwise position. Figure 3.7 shows the peak levels of RMS unsteady excitation on the fin at 43.5° angle of attack (peak buffeting) for the low wing baseline against fin chordwise location at a spanwise location corresponding to tapping 6. The location chosen to show the unsteady pressures at 5% chord represents the ideal location in terms of maximising the signal to noise ratio. The measured magnitudes of unsteady pressure are greater than other published work on fin buffet, generally completed at fin locations aft of 5% chord. The mechanism of this interaction of the flow with the fin is under further investigation.

Fin buffeting of alternative fuselage shapes

Figure 3.8 compares the fin buffeting response from the low wing baseline, pentagonal, and chine fuselage sections. It is clear that the response with the different fuselage shapes differ in both magnitude and shape. The onset angle of attack for chine and pentagonal forebody shape is advanced compared to the low wing baseline configuration, with the unsteady flow impinging onto the fin at a lower angle of attack.

Figure 3.9 illustrates the motion of the wing and forebody vortices resulting from the velocities induced by each other. The forebody vortex and wing vortex will have the effect of wrapping around each other, with the wing vortex moving inboard and over the top of the forebody vortex while the forebody vortex will be dragged down to the wing surface and underneath the wing vortex. Any increase in the forebody vortex strength will enhance this interaction, with the wing vortex being dragged further inboard than for a weak forebody vortex. Figure 3.10 shows flow visualisation for the low wing baseline compared to the chine fuselage for an angle of attack of 26°. The low wing baseline is associated with a relatively weak forebody vortex compared to the chine vortex. At this angle of attack, the chine vortex becomes wrapped around the wing vortex, resulting in a large shift inboard of the wing vortex, whereas the inboard shift for the low wing baseline is much smaller by virtue of the weaker forebody vortex.

With an increased forebody vortex strength, for similar planforms, the wing vortex will contact the fin at an earlier angle of attack. This is evidenced from the fin

buffeting response shown in figure 3.8, where the buffeting onset angle of attack is changed with fuselage shape. The weak forebody vortex associated with the low wing baseline results in a dalayed buffeting onset angle compared to the pentagonal and chine fuselage, both of which will possess stronger forebody vortices.

The influence of the geometry on the unsteady flow impinging on the fin is further evidenced when examining the high wing baseline and triangular fuselage fin buffeting response of figure 3.11. These two configurations are geometrically similar with the triangular forebody producing a much stronger forebody vortex than the square forebody of the high wing case. There is a large reduction in the fin buffeting onset angle for the triangular forebody compared to the high wing configuration resulting from the strong forebody vortex moving the wing vortex inboard to impinge on the fin at a lower angle of attack.

If the fin buffeting onset angle of attack is changed, for a fixed tunnel speed and wing planform, there is a change in the modified reduced frequency parameter. A reduction of onset angle of attack can be considered as equivalent of a lower sweep angle for the wing and hence a reduced n_m (figure 1.1). For a fixed angle of attack and test speed, according to the reduced frequency parameter, the excitation frequency will be reduced as n_m reduces. Figure 3.12 compares the spectra of the unsteady pressure for the triangular and high wing baseline configurations at an angle of attack of 42.6° corresponding to peak buffeting of the high wing baseline configuration. It is relevant to note that this configuration is untuned from the fin modal frequency resulting in a reduced magnitude of buffeting response. The characteristic frequency associated with the triangular forebody is, as predicted, significantly lower.

In summary it is clear that,

- The influence of fuselage shape is to modify the angle of attack that the unsteady flow first impinges on the fin to change the buffeting onset angle of attack. Configurations associated with stronger forebody vortices will exhibit a lower onset angle of attack.
- Stronger forebody vortices which result in changes in the flow geometry also reduce the modified frequency parameter for the same wing planform. At a fixed angle of attack, the characteristic frequency of the unsteady flow is reduced as the forebody vortex strength increases

Figure 3.13 shows the spectra of unsteady pressure associated with the chined fuselage shape for pre peak, peak and post buffeting conditions. Clearly evident is the existence of two peaks in the pressure spectra. This is further illustrated in the contour plot of figure 3.14. PSD's have been calculated at a range of angles of attack and combined to show the spectral magnitude as contour levels. The dots on the figure are representative of the data points used to create the plot. This presentation technique summarises an extensive amount of information into a single figure and can be used to compare configurations. The double spectral peak of the chine section is clearly visible and provides a marked contrast with figure 4.15 showing the spectra of the high wing baseline configuration, which posesses only a single dominant frequency in the excitation. This effect is characteristic of the chine fuselage section and the subject of further investigation.

Conclusions

Unsteady excitation must be present on the fin to produce a response. For single fin buffeting the majority of excitation occurs toward the fin tip and fin leading edge. Studies which consider these locations will be associated with the high signal to noise ratios.

The geometry of the unsteady excitation defines the condition of buffeting onset, where the vortical shear layers first impact the fin. A critical condition is reached when the vortical shear layers meet at the fin tip, resulting in peak excitation. Under these conditions of maximum excitation, maximum response occurs when the dominant frequency within the excitation is tuned to a response mode. A change in test speed will result in a change in this characteristic frequency and a consequential reduction in the fin buffeting response. This shows the importance of tuning the unsteady excitation to a response mode to establish the most severe fin buffeting condition.

The fin buffeting response associated with alternative fuselage shapes is the result of changes in the geometry of the flow and/or the characteristic frequency. Increases in the strength of the forebody vortex will drag the wing vortex inboard compared to that associated with a weak forebody vortex. The vortical shear layers will contact the fin at a lower angle of attack and advance the buffeting onset condition.

The change in the geometry of the flow relative to angle of attack effectively modifies the reduced frequency parameter such that for a given angle of attack, the frequency of excitation will be reduced. This will modify the response of the fin as a function of the dominant frequency within the excitation relative to a fin mode. This particularly apparent around the peak buffeting condition. Experimental or flight test results which include configurational changes should consequently be treated with some care.

Acknowledgements

The authors would like to acknowledge the support of British Aerospace Defence, Military Aircraft Division, Warton under Agreement KAP04FAAC/KPP04GAAC and the EPSRC

References

1. Lang J D and Francis M S, Unsteady Aerodynamics and Dynamic Aircraft Manoeuvrability, AGARD CP-386, April 1985
2. Herbst W B, Dynamics of Air Combat, Journal of Aircraft, Vol 20, No 7, pp 594-598, July 1983
3. Hamilton B I L, The operational problems encountered during precise manoeuvring and tracking, AGARD AR-82, July 1975
4. Hanson P W, Structural and Aerodynamic quantities of the dynamic system, similarity laws, and model testing, AGARD AR-82, July 1975
5. Mabey D G, Some aspects of aircraft dynamic loads due to flow separation. AGARD R-750, February 1988
6. Ferman M A, Patel S R, Zimmerman N H and Gerstenkorn G. A Unified Approach to Buffet Response of Fighter Aircraft Empennage, AGARD CP-483, April 1990
7. Martin C A and Thompson D H, Scale Model Measurements of Fin Buffet Due to Vortex Bursting on F/A-18. AGARD CP-497, May 1991
8 Nelson R C, Unsteady Aerodynamics of Slender Wings, AGARD-R-776, April 1991
9. Gursal I, Unsteady Flow Phenomena over Delta Wings at High Angle of Attack. AIAA Journal, Vol 32, no 4, pp 225-231, February 1994
10. Bean D E and Wood N J, An Experimental Investigation of Twin Fin Buffeting and Suppression. AIAA 93-0054, Presented at the 31st Aerospace Sciences Meeting and Exhibit, Reno, Nevada, January 1993
11. Mabey D G, Measurements of Fin Buffeting on an 'F-18' Model and a Derived Interpretative Hypothesis. DRA Technical Memorandum, AERO 2224, September 1991
12. Bean D E, A study of Reduced Frequency Parameter for Fin Buffeting Response on Slender Delta Configurations. Final Report 2112/096/A, DRA Bedford
13. Norris G. New technique speeds wing design, Flight International. p 26, 6-12 March 1996
14. Mabey D G, Some Aspects of Aircraft Dynamic Loads due to Flow Separation, AGARD R-750, February 1988

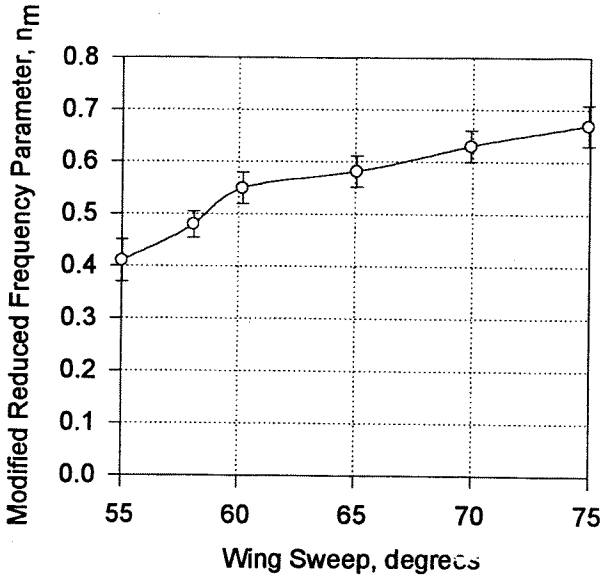

Figure 1.1 - Effect of wing sweep angle on reduced frequency parameter

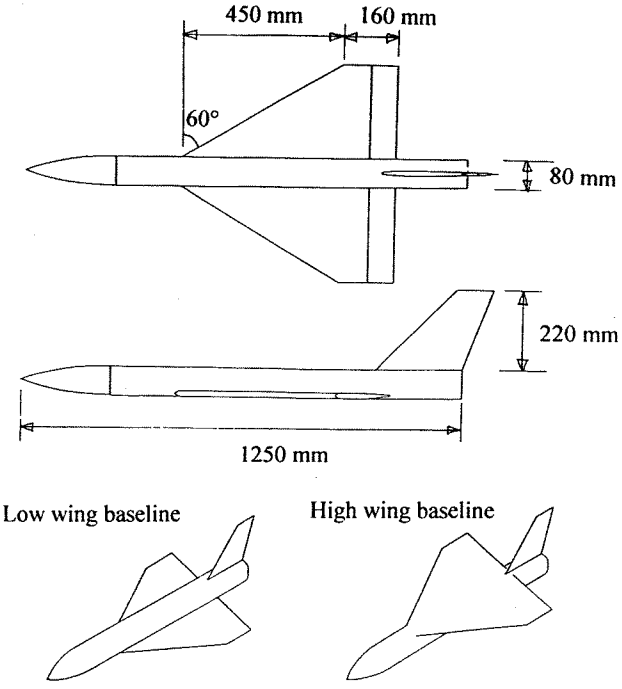

Figure 2.1 - Baseline low wing wind tunnel model

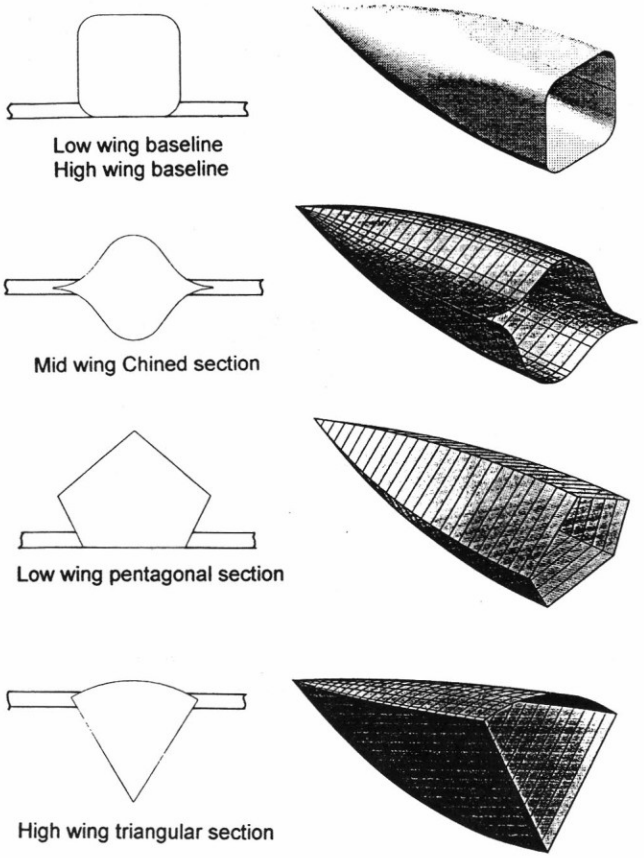

Figure 2.2 - Alternative fuselage cross sections

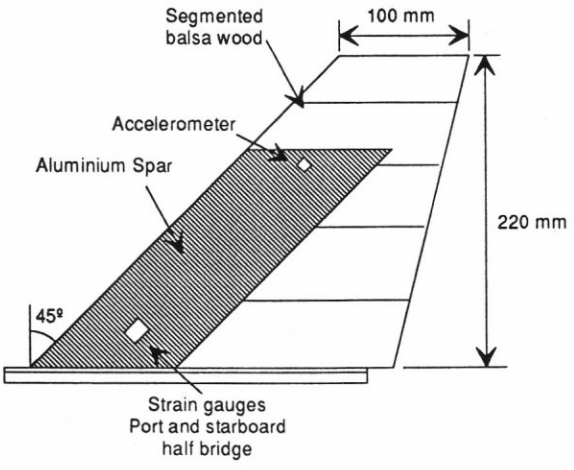

Figure 2.3 - Flexible fin

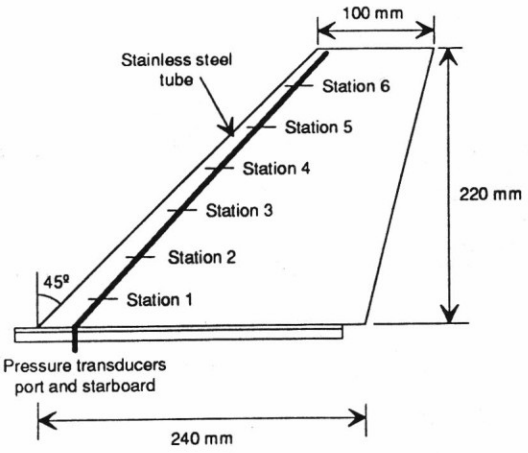

Tapping number	Height from fin root /mm
1	25
2	60
3	95
4	130
5	165
6	200

Figure 2.4 - Rigid pressure tapped fin

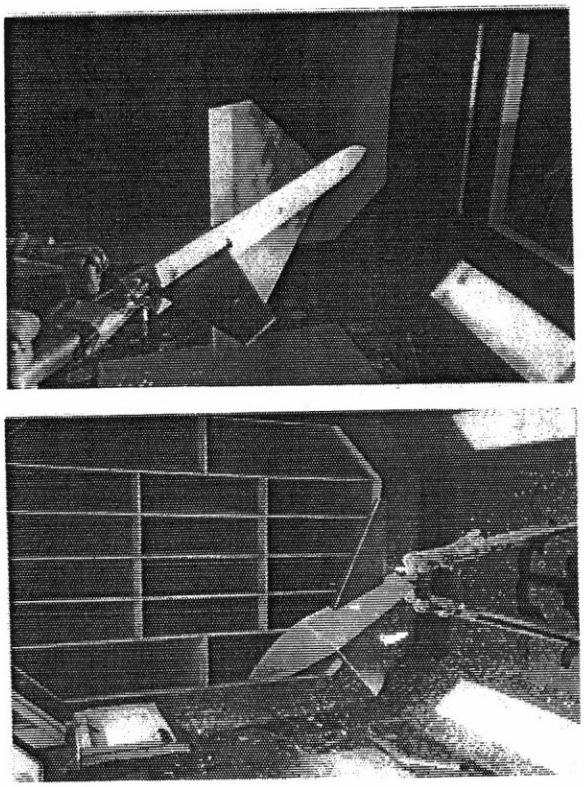

Figure 2.5 Model installation in wind tunnel

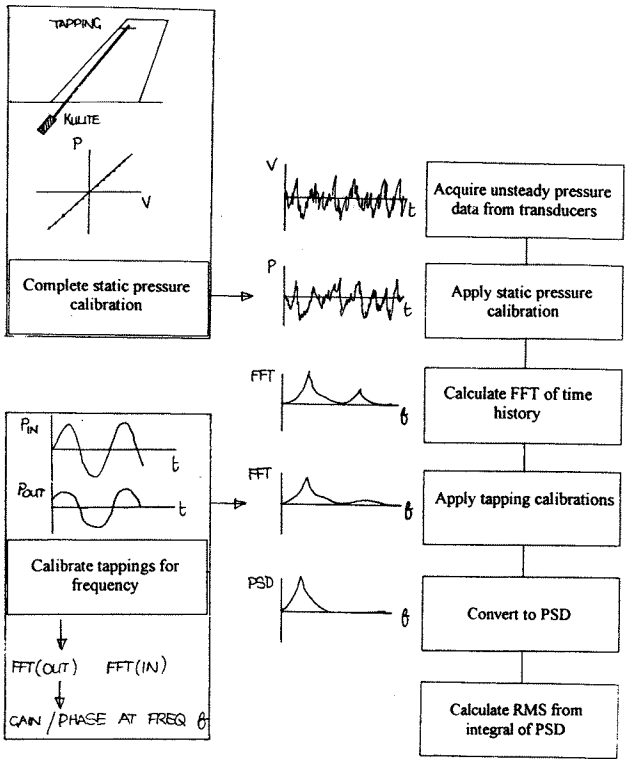

Figure 2.6 - Data processing sequence

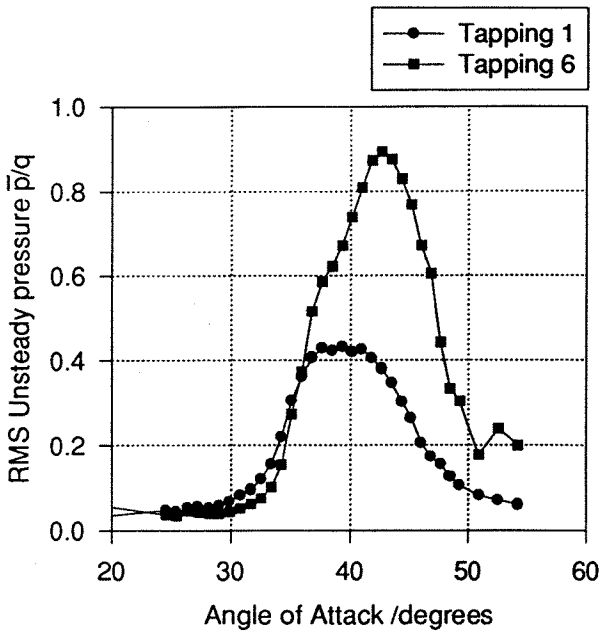

Figure 3.2 - RMS unsteady pressure on fin low wing baseline

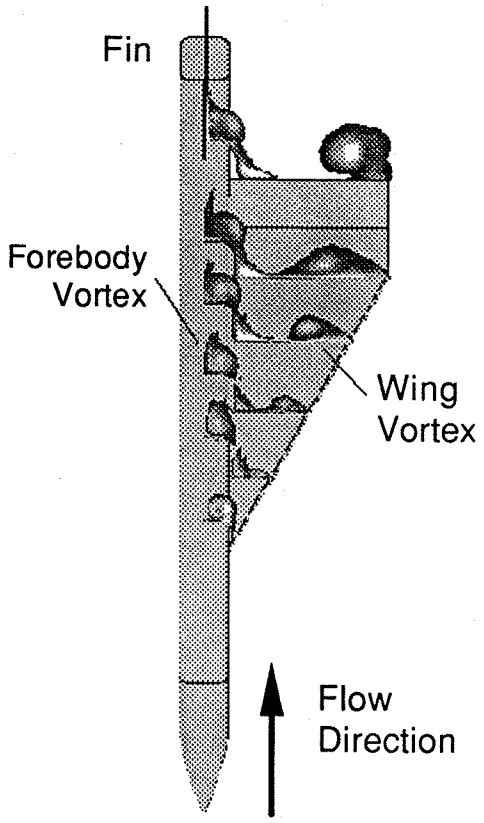

Figure 3.1 - Low wing baseline flow features

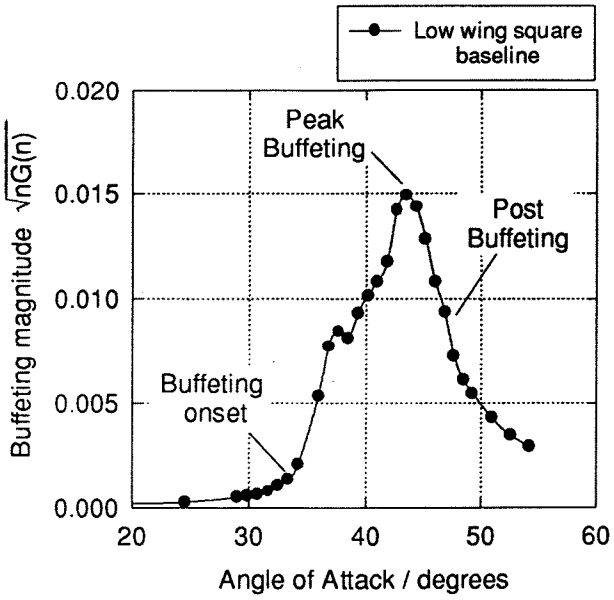

Figure 3.3 - Fin buffeting of baseline configuration

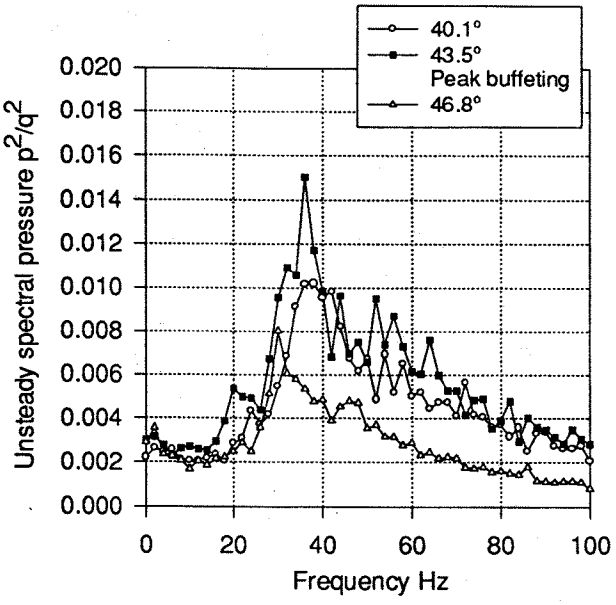

Figure 3.4 - PSD's of low wing baseline

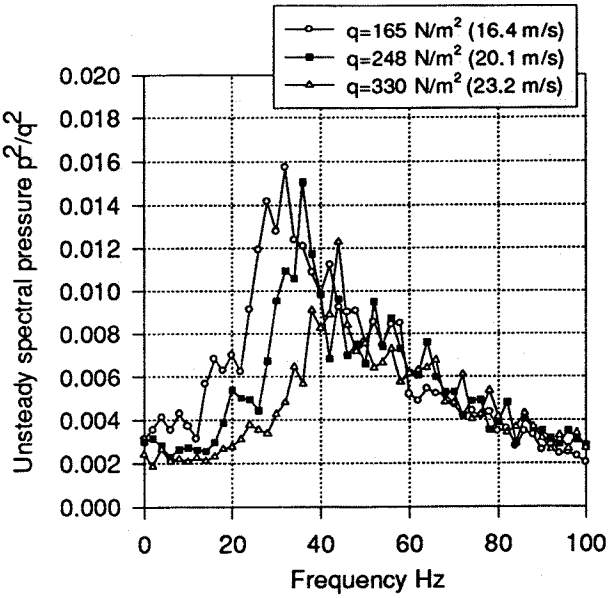

Figure 3.6a - Effect of speed on unsteady pressure spectra - Frequency

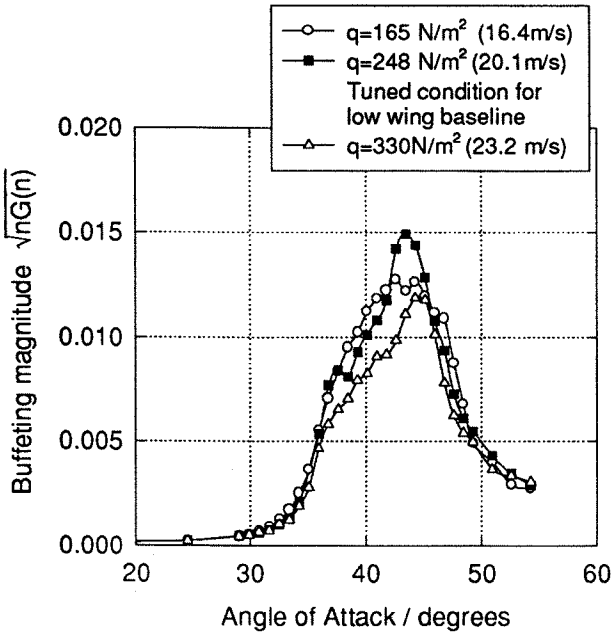

Figure 3.5 - Effect of speed on fin buffeting

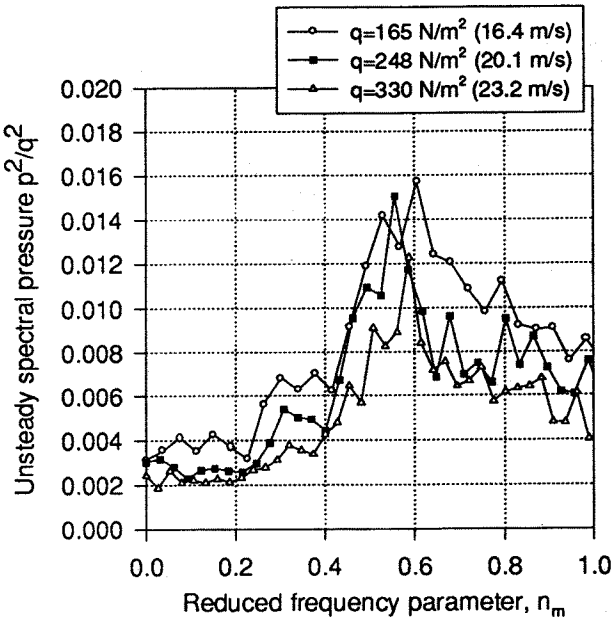

Figure 3.6b - Effect of speed on unsteady pressure spectra - Reduced frequency parameter

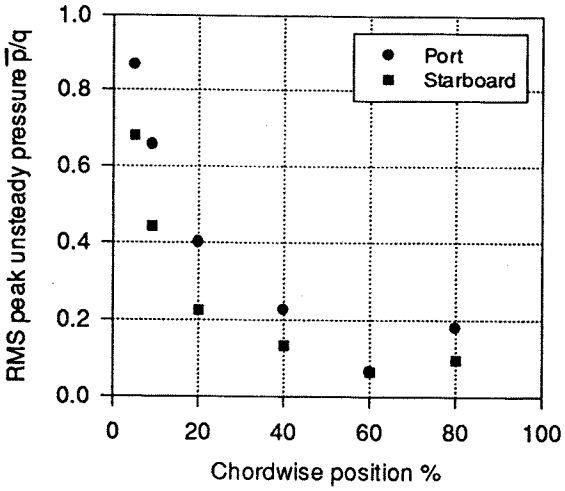

Figure 3.7 - Distribution of unsteady pressure on fin

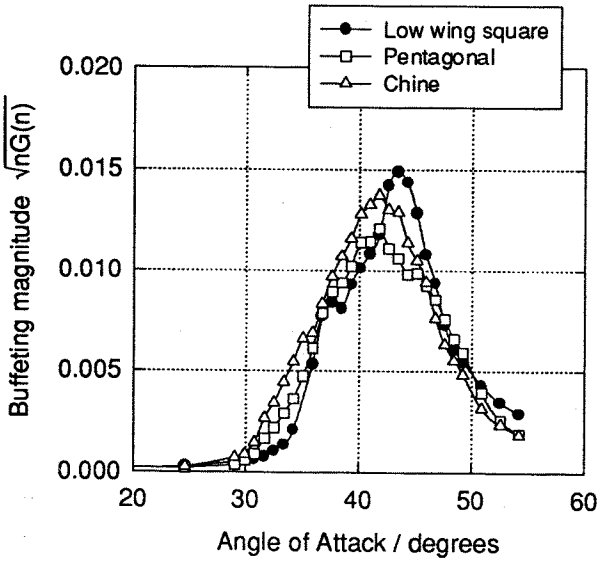

Figure 3.8 - Effect of forebody shape on fin buffeting

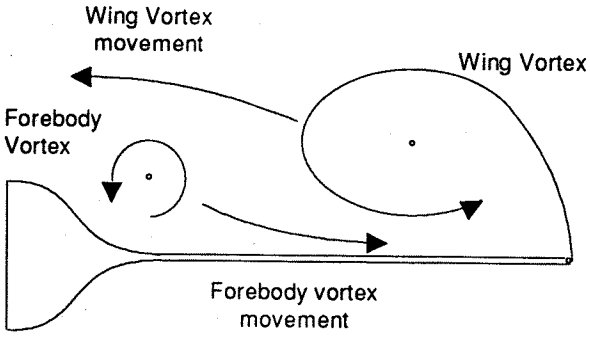

Figure 3.9 - Forebody/vortex wing interaction with increasing vortex strength

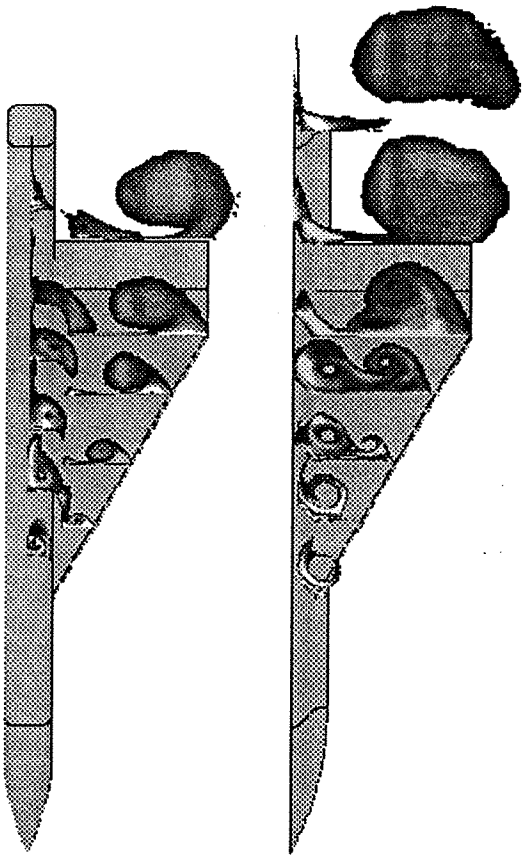

Figure 3.10 - Effect of forebody shape on vortex geometry

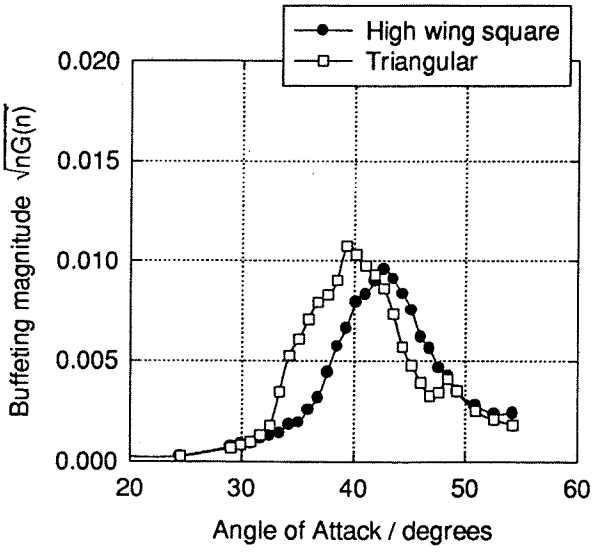

Figure 3.11 - Comparison of square and triangular buffeting

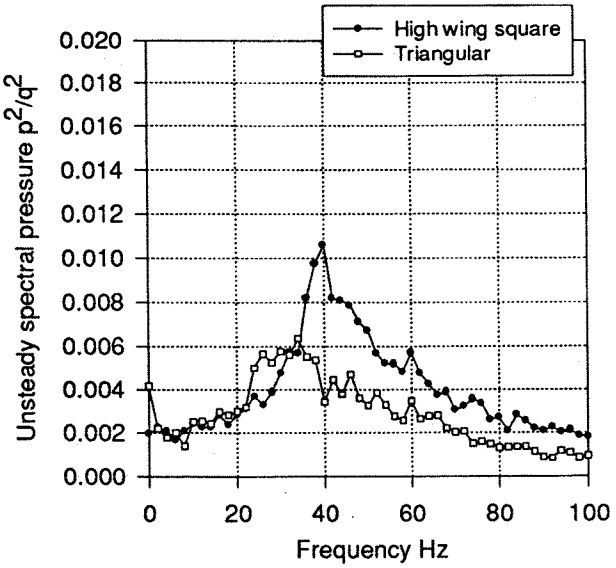

Figure 3.12 - Comparison of high wing square and triangular PSD's

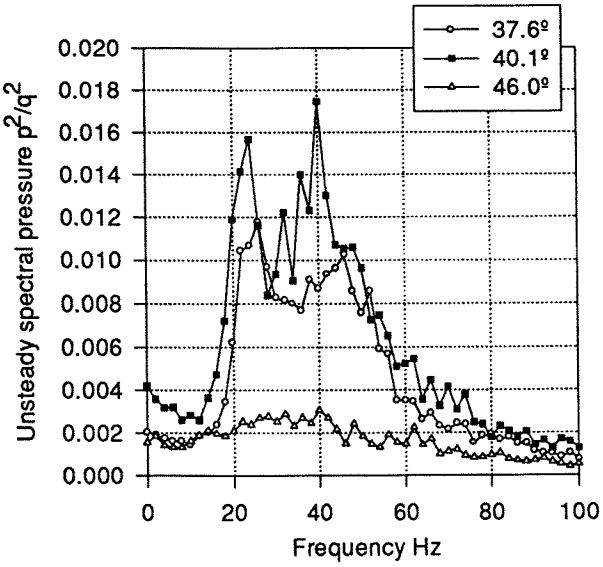

Figure 3.13 - Spectra of unsteady pressure for chine fuselage

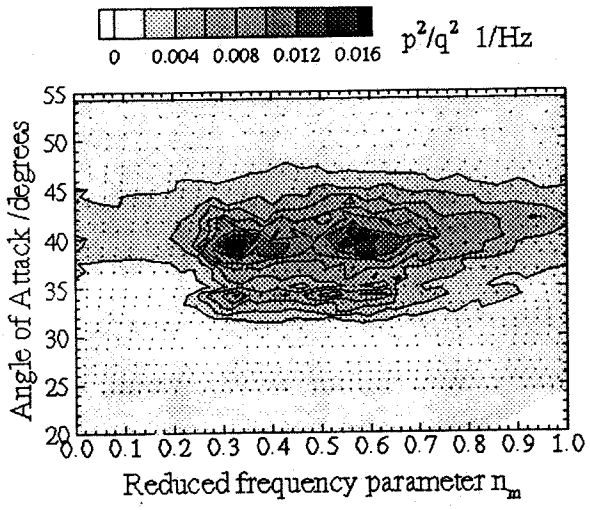

Figure 3.14 - Contour of unsteady pressure for chine forebody

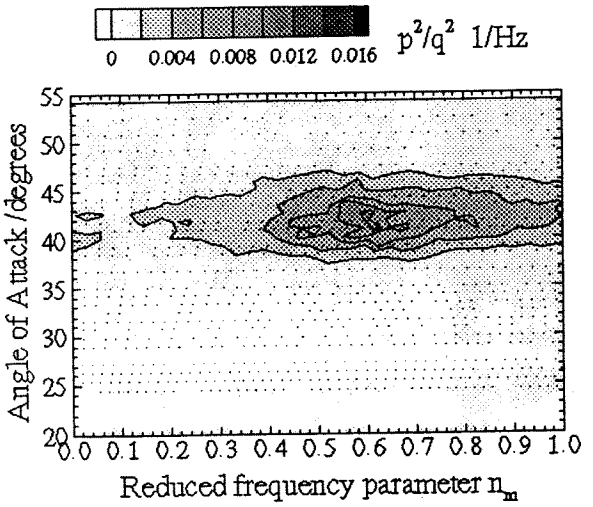

Figure 3.15 - Contour of unsteady pressure for high wing square fuselage